Quantifying Rotations of Spheric Objects

Alexander Szep
Vienna University of Technology, Institute of Computer Technology
Gusshausstr. 27-29 / 384, A-1040 Vienna, Austria
alexander.szep@tuwien.ac.at

Abstract

This work presents an approach to quantify rotations of spheric objects with a single camera. We apply this method to objectively classify racket sports equipment. Therefore, we observe the ball impact on a racket and compare differences in rotations quantified prior to and after the impact. Our approach combines motion segmentation with tracking both the ball center and corners of the surface texture. A 2D warping of these corner positions reveals the rotation. We neither require a motion model nor any user intervention. Experimental results verify our approach and prove the feasibility of our application scenario based on visual rotation quantification.

1 Introduction

We present a visual method for quantifying rotations of spheric objects aimed for the ball sports domain. Knowledge about ball rotation enables a range of applications for sports where rotation plays a crucial role like in table tennis, tennis, soccer, baseball, golf, bowling, and billiard. Three envisioned application domains in racket sports motivate us: Our primary domain is racket equipment classification (*Domain-1*). The amount of rotation (spin) a racket imparts on a ball is a significant classification factor. Such classifications can be used in two ways: First, athletes can make objective and deliberate decisions to purchase equipment. Second, sports federations can classify illegal equipment which does not conform to the rules. *Domain-2* is training feedback analysis. Feedback based on ball spin is a useful pointer to improve an athlete's technique. *Domain-3* are virtual replays for television broadcasts of ball sports events. Showing spectators significant ball spin characteristics in virtual replays makes a sport more "tangible" and thereby potentially arouses more interest in the audience. This work focuses only on equipment classification (Domain-1). However, the other two domains are clear long-term goals even though their realization requires a new approach.

Whereas numerous work (such as e.g. [1], [2], and [3]) has been done focused on ball tracking to obtain trajectory paths less past work has dealt with ball spin analysis. Previous work on spin analysis was done in following sports domains: tennis [4], soccer [5], table tennis [6], and baseball [7]. The authors of [4] measure the spin of tennis balls based on high-speed image sequences but favor manual spin measurement over computer vision methods because of higher accuracy. Neilson *et al.* [5] measure the spin of a soccer ball. Their results are based on a unique color pattern on the ball surface where each 2D view of the ball identifies its 3D position. Our approach in contrast works with arbitrary surface features. Tamaki *et al.* [6] measure ball spin of table tennis balls. Their approach is based on image registration in addition to depth information from a manually fitted 3D sphere model. The work of Boracchi *et al.* [8] examines spin by analyzing blurred images. For the general case of a spinning and translating ball they propose a semi-automatic user-assisted approach. Both [6] and [8] require manual user intervention whereas our approach is fully automatic. Theobalt *et al.* [7] determine the spin of baseballs based on multi-exposure stereo images. Their approach relies on 3D depth data of predefined tracked color markers. We instead only use a single camera and do not need depth information.

Our contribution is a fully automated spin measurement without user intervention. High-speed cameras, as used in our acquisition setup, usually deliver gray scale image data. Therefore, our method relies solely on arbitrary gray scale images. We provide measurement results within less than three seconds for 20 processed frames—sufficient for the racket classification application. Further, our method is independent from any motion model and works with uncalibrated, monocular camera data. We point out that we only measure spin with a rotational axis perpendicular to the image plane—this renders our approach inappropriate for assessing spin in real game rallies. Although ball trajectory analysis reveals additional discriminative data for racket classification we neglect it in this paper and focus solely on spin measuring.

We explain our video data acquisition setting in Section 2 followed by implemented method details in Section 3. In Section 4 we present and discuss experimental results and compare them to existing approaches. Finally, we revise our contribution and give an outlook in Section 5.

2 Video Data Acquisition

We use rotating table tennis balls as a test environment. Compared to tennis, soccer, baseball, and golf we can reproduce and verify results with less effort due to a simpler data acquisition setting, depicted in Figure 1. A similar setting with a rigidly mounted racket is described in [4]. We use an automatic ball feeder (on the left in the figure) to obtain repeatable preconditions. The feeder propels the balls with backspin (3800 ± 100 revolutions per minute (rpm)) towards the rigidly mounted racket from a short distance (0.5 m)—we capture the ball before and after impact on the racket with a high-speed camera. The image plane is parallel to the translational ball motion and the camera observes the ball from 2 m distance (focal length 100 mm). We light the scene with three 1000 W floodlights to achieve enough contrast on the ball contour and on the ball surface features for further processing.

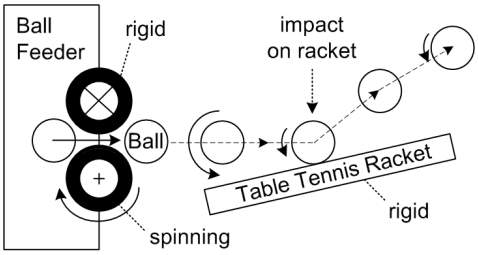

Figure 1. Video data acquisition setting

The main light direction of all three floodlights is positioned perpendicular to the image plane. The frame rate is 1000 frames per second (fps), the exposure time is $\frac{1}{7000}s$ to minimize motion blur, and the captured image sequences have a resolution of 1280×512 pixels (landscape). Every certified table tennis ball has a printed logo of the manufacturer on its surface. This logo might be occluded in our acquisition setup. Therefore, we augment the ball surface with additional painted artificial features to ensure visible texture in every captured frame.

3 Spin Calculation

Figure 2 depicts the spin calculation principle with four superimposed ball images taken at four subsequent times of a sequence—the ball moves from left to right as in Figure 1. The first two frames at the left are taken prior to the ball impact whereas the last two frames at the right are taken after the impact. The spin calculation is based on tracking of ball surface features—we mark a particular corner of such a tracked feature with yellow dots for better visibility (this yellow dot only augments Figure 2 and does not exist on the ball itself). Blue dashed lines mark the ball center positions and solid red lines connect the tracked yellow dot with the corresponding ball center. Two red lines span a certain angle within an elapsed time (denoted with α and β in Figure 2). The spin corresponding to such spanned angles results from Eq. (1):

$$spin = \frac{angle_{spanned}}{time_{elapsed}} \cdot \frac{60s}{360°}. \quad (1)$$

The scale factor at the end ensures the unit of rpm—we divide by 360° to obtain complete revolutions and multiply with 60 seconds to obtain revolutions per minute. The angle $\alpha = 137°$ in Figure 2 results from the left two ball images (prior to the impact) within an elapsed time of $6/1000s$ and equals a spin of 3806 rpm. The angle $\beta = 18°$ is calculated after the impact based on the right two ball images within $20/1000s$, so the spin equals to 150 rpm.

Before we can apply Eq. (1) for spin calculation, we need to process the image sequences. Our processing pipeline consists of the following five steps:

Step 1: Segmenting ball from background: To do this, we learn a background model based on frames before a ball becomes visible in the scene. During this learning phase we observe a certain intensity range for each image pixel. After the learning phase a pixel is considered as foreground when this pixel's intensity value is outside the learned intensity range. This segmentation method is implemented in *OpenCV*.

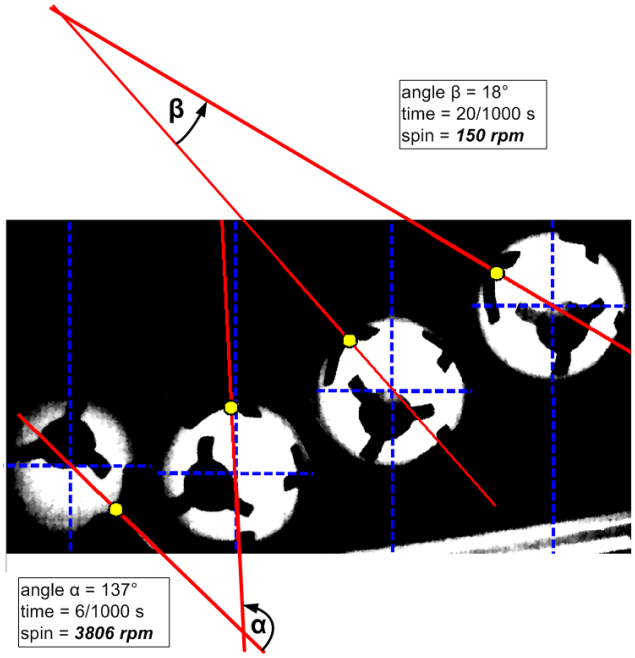

Figure 2. Spin calculation principle

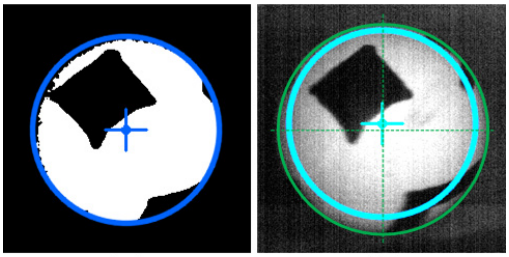

Figure 3. Circle fitting to ball contour

Step 2: Determining center position: First, we fit a bounding box around the segmented ball contour. Next, we fit a circle into this bounding box—the circle center corresponds to the ball center. Figure 3a shows a segmented input image with a superimposed fitted circle and the ball center. Figure 3b highlights a problem: If the ball surface is not lit uniformly, as in our case, the contrast varies between the imaged sphere contour and the background. This hinders accurate circle fitting and center finding (compare the determined smaller circle and the true larger circle).

Step 3: Identifying corners within our region of interest (ball contour): According to the criterion for "good" corners in [9] we identify corners where both eigenvalues of the second moment matrix are above a certain threshold. We set the threshold to 80% of the best found corner's lower eigenvalue. This threshold has been evaluated empirically and ensures "good corner quality".

Step 4: Tracking identified corners between consecutive frames: We apply the Kanade-Lucas-Tomasi algorithm [10] for tracking corresponding corners.

Step 5: Calculating a rotation angle by 2D warping of surface feature positions: Figure 4 explains the calculation of the rotation angle based on the (inner) vector product. Consider the two circles as abstracted ball images of Figure 2 with a black and a white square

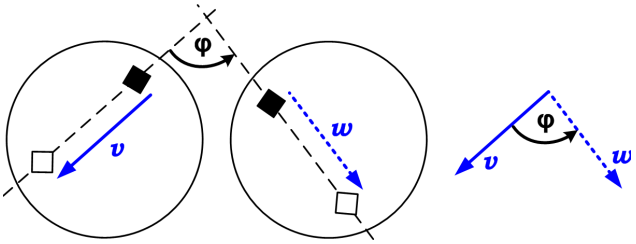

Figure 4. Angle calculation

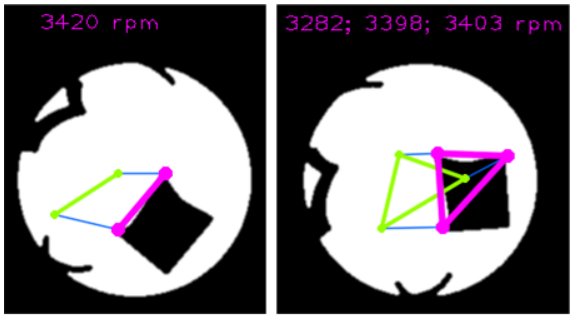

Figure 5. Corner tracking (synthetic images)

representing two surface features. These features are connected by straight edges (dashed lines) and we assume the features retain their spatial relation on the ball surface (rigid body assumption). We denote the direction from the black to the white square in the left ball image as vector $\vec{v}$ and the direction from the black to the white square in the right ball image as vector $\vec{w}$ ($\vec{v}, \vec{w} \in \Re^2$). Based on the inner vector product, the angle φ is calculated according to Eq. (2):

$$\varphi = arccos\left(\frac{\vec{v} \cdot \vec{w}}{\|\vec{v}\| \cdot \|\vec{w}\|}\right). \qquad (2)$$

After we obtained the rotation angle, we can apply Eq. (1) to calculate the corresponding spin.

4 Results and Comparison

Obtaining ground truth data from real image sequences is a tedious task. Therefore, we generated synthetic image sequences where ground truth is known. Figure 5 visualizes two snapshots of an analyzed synthetic image sequence. In Figure 5a two corners of the square-like region are automatically chosen and tracked—the magenta line connects the corners in the current frame whereas the green line shows the relation of these corners in the previous frame (thin blue lines mark corresponding corners). The top of the image contains the calculated corresponding spin value. In comparison thereto, in Figure 5b three corner correspondences are tracked and therefore we can calculate three spin values. Ideally, all three values should be the same, the differences between them indicate inaccuracies in the location of corresponding corners.

Figure 6 shows the calculated spins of the synthetic sequence. Ground truth spin is 3667 rpm prior to impact and 417 rpm after impact, marked with blue lines. Measured values are marked with magenta circles. The

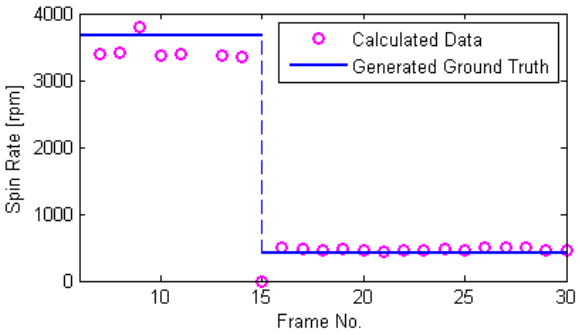

Figure 6. Results of synthetic sequence

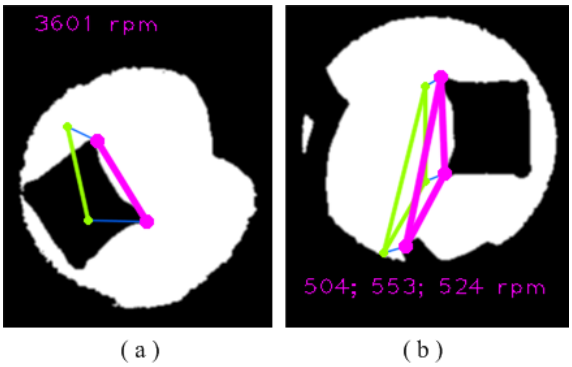

Figure 7. Corner tracking (real images)

spin value zero at frame 15 is due to the simulated impact with momentarily zero motion. The values in this diagram represent average values calculated over the number of tracked corner correspondences—with reference to Figure 5b this is an average over three values. Of course this simple averaging includes also outliers but we want to show the mean error variation. Disregarding outliers, the mean measurement error prior to impact is -8% and after impact +3%.

Figure 7 depicts two snapshots of an analyzed real image sequence—in part a two corners are tracked, whereas in part b three corners are tracked (current corner positions are magenta, previous positions are green). Between Figure 7 and Figure 5 we notice the apparently less smooth ball contour shapes of the real snapshots. This results from varying contrast between the projected real ball contour and the background.

Figure 8 shows the calculated spins of the real sequence. We obtain the ground truth by manually measuring angle differences between corresponding corners in the sequence on a computer display. The spin prior to impact is 3750 rpm and after impact 500 rpm. Disregarding outliers, the mean measurement error prior to impact is -7% and after impact -3%—so absolute errors of synthetic and real sequences are comparable.

Remark: Both Figures 6 and 8 show outliers at frame numbers 9 and 12 respectively. At these positions only one corner instead of at least two sufficiently "good" corners could be revealed. However, to obtain a spin value for each frame, we replaced one (non-existing) corner position by the ball center position. Spin calculation based on the center position and one surface corner is not as robust as the proposed method with

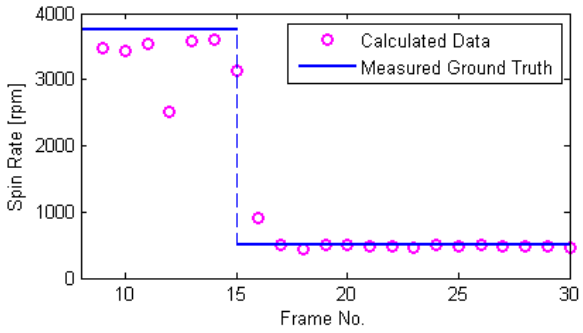

Figure 8. Results of real sequence

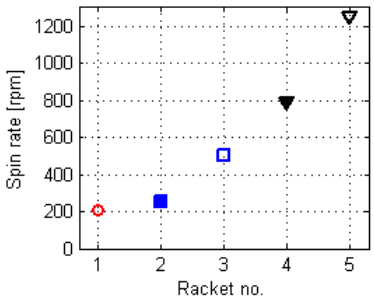

Figure 9. Spin responses of five different rackets

at least two surface corners—the center position cannot be determined as accurately as a corner (compare Figure 3).

We captured sequences with five different rackets with results similar to Figure 6 and Figure 8 (these measurements are not shown in detail). We call the measured spin of a racket after impact its *spin response* to a certain spin before impact. Measured spin responses revealed an average range per sequence between 200 and 1250 rpm depending on the racket. Figure 9 illustrates these measurements where racket no. 3 corresponds to results of Figure 8 after impact. In the case of these five rackets the spin response is discriminative enough to uniquely distinguish between them.

To reveal our strengths and limitations we compare our results with two approaches ([8], [7]): The blur approach of Boracchi *et al.* [8] requires a feature to have an observed angle displacement of at least 3.6°—our method does not have a lower bound. In [8] the authors assessed only cases without translation where the mean error was 3 - 11% for a spin range 833 - 1666 rpm. In contrast to them we cope with additionally superimposed translations. Theobalt *et al.* [7] state an error of 0.4 - 2.5% for spins of 1258 - 1623 rpm for their stereo based approach. In contrast to both approaches we cope with a larger spin range between 0 - 3750 rpm. On the other hand our mean error magnitude can increase to about 8%.

5 Conclusion and Outlook

We have shown a motion analysis approach focused on the measurement of ball spin. Experiments proved different spin responses on different rackets which makes this method's results feasible for racket classification based on spin measurements. A sequence of 20 captured frames is sufficient for a significant racket classification. The execution time for processing 20 frames is about 3 seconds (run on an Intel Core i7 L620, 2 GHz processor)—this delay is acceptable for an application like on site classification of illegal rackets during sport events. However, the same delay might be an upper limit for application domains like training feedback and virtual replays for sports broadcasts.

We identify two major future steps:

- Most importantly, we strive for quantifying rotation without restrictions on the spin axis position. Hence, to enable other long-term application domains such as training feedback analysis and virtual replays, the development of a new approach is crucial.
- Our method should be sufficiently robust to measure spin based on any two subsequent frames. We will successively challenge our method by decreasing the number of artificial surface features.

Acknowledgements

We owe thanks to Professor Arnold Baca and Philipp Kornfeind who enabled the data acquisition at the Department of Biomechanics, Kinesiology and Applied Computer Science (University of Vienna).

References

[1] T. Kim, Y. Seo, and K.-S. Hong, "Physics-based 3d position analysis of a soccer ball from monocular image sequences," in *Sixth International Conference on Computer Vision (ICCV'98)*, pp. 721–726, Jan. 1998.

[2] G. Pingali, A. Opalach, and Y. Jean, "Ball tracking and virtual replays for innovative tennis broadcasts," in *International Conference on Pattern Recognition (ICPR'00)*, pp. 152–156, 2000.

[3] A. Guéziec, "Tracking pitches for broadcast television," *IEEE Computer*, vol. 35, pp. 38–43, Mar. 2002.

[4] S. R. Goodwill and S. J. Haake, "Ball spin generation for oblique impacts with a tennis racket," *Experimental Mechanics*, vol. 44, no. 2, pp. 195–206, 2004.

[5] P. Neilson, R. Jones, D. Kerr, and C. Sumpter, "An image recognition system for the measurement of soccer ball spin characteristics," *Measurement Science and Technology*, vol. 15, no. 11, pp. 2239–2247, 2004.

[6] T. Tamaki, T. Sugino, and M. Yamamoto, "Measuring ball spin by image registration," in *Proceedings of the Tenth Korea-Japan Joint Workshop on Frontiers of Computer Vision*, pp. 269–274, 2004.

[7] C. Theobalt, I. Albrecht, J. Haber, M. Magnor, and H.-P. Seidel, "Pitching a baseball - tracking high-speed motion with multi-exposure images," in *Proceedings of ACM SIGGRAPH*, 2004.

[8] G. Boracchi, V. Caglioti, and A. Giusti, "Estimation of 3d instantaneous motion of a ball from a single motion-blurred image," in *VISIGRAPP*, pp. 225–237, 2009.

[9] J. Shi and C. Tomasi, "Good features to track," in *IEEE Conference on Computer Vision and Pattern Recognition (CVPR'94)*, pp. 593–600, 1994.

[10] C. Tomasi and T. Kanade, "Shape and motion from image streams under orthography: a factorization m.," *Int. Journal of Computer Vision (IJCV)*, vol. 9, no. 2, pp. 137–154, 1992.